ChemComm

COMMUNICATION

View Article Online
View Journal | View Issue

Cite this: *Chem. Commun.*, 2016, 52, 12618

Received 28th June 2016,
Accepted 28th September 2016

DOI: 10.1039/c6cc05362a

www.rsc.org/chemcomm

A comparative study of graphite electrodes using the co-intercalation phenomenon for rechargeable Li, Na and K batteries†

Haegyeom Kim,‡[a] Gabin Yoon,[ab] Kyungmi Lim[a] and Kisuk Kang*[ab]

Here, we demonstrate that graphite can serve as a versatile electrode for various rechargeable battery types by reversibly accommodating solvated alkali ions (such as K, Na, and Li) through co-intercalation in its galleries. The co-intercalation of alkali ions is observed to occur *via* staging reactions. Notably, their insertion behaviors, including their specific capacity, are remarkably similar regardless of the alkali ion species despite the different solubility limits of K, Na, and Li ions in graphite. Nevertheless, the insertion potentials of the solvated alkali ions differ from each other and are observed to be correlated with the interlayer distance in the intercalated graphite gallery.

Graphite has been used as a commercial anode material for Li-ion batteries (LIBs) because of the reversible Li de/intercalation that can occur in the host. Its high specific capacity ($\sim LiC_6$) and low operation voltage combined with low cost and non-toxicity have made graphite one of the most successful anode materials for LIBs to date.[1–3] Recent studies have revealed that graphite is also capable of accommodating a large amount of K ions by forming the KC_8 compound in K-ion batteries (KIBs).[4–6] In KIBs, the graphite anode can deliver a reversible capacity of $\sim$250 mA h g^{-1} with an average voltage of 0.2 V (*vs.* K/K^+). However, a similar alkali ion, Na^+, cannot be intercalated into the graphite host. The lack of the capability to store Na^+ ($Na\delta C$ ($\delta \sim 0$)) prohibited the use of graphite as an anode for Na-ion batteries (NIBs) for many years.[7,8] Moreover, no stable Na–C binary compound has been identified to date. These distinct behaviors of alkali ion insertion into graphite have led to significantly different electrochemical performances of graphite electrodes in LIBs, NIBs, and KIBs, *i.e.*, $Li_{1/6}C$, $Na\delta C$ ($\delta \sim 0$), and $K_{1/8}C$, respectively.[8–11] Recently, our group as well as other groups demonstrated that graphite can accommodate Na ions reversibly in its galleries when linear ether solvents are used.[12–17] The reaction was observed to involve the co-intercalation of both Na ions and ether molecules in the form of solvated Na ions into the graphite.[13] It was also revealed that the intercalation of the solvated Na ions can be fast, comparable to Li ion intercalation in graphite. Moreover, the intercalation voltage varies with the selection of solvent unlike conventional intercalation, implying that the nature of the intercalation of solvated ions may be intrinsically different from that of typical ion intercalation.[13–15] These prior observations indicate the presence of a complex interaction among the guest ions, solvent molecules, and the graphite host during the intercalation. Unveiling the correlations among these components would extend our understanding of the intercalation chemistry, the key fundamental reaction in modern rechargeable batteries, and hint at an effective strategy to utilize graphite as a versatile host material for various rechargeable batteries.

In this work, we explore the intercalation chemistry of various solvated alkali ions (M = Li, Na, and K) in graphite and report that Li and K ions can also be intercalated in the form of solvated complex ions when the solvent molecule is properly selected. The use of an ether-based electrolyte enables the co-intercalation of both Li and K ions into the graphite at significantly different intercalation voltages than those of the known LiC_6 or KC_8 compound formation. Structural investigation of the co-intercalation using *ex situ* X-ray diffraction (XRD) reveals that the same staging behavior is observed regardless of the alkali ion species. However, the insertion potentials of the solvated alkali ions (*vs.* the normal hydrogen electrode (NHE)) are different and related to the distance between graphene layers in the discharged state.

The electrochemical properties of the co-intercalating graphite electrode were examined in Li, Na, and K half-cell configurations, in which each alkali metal (Li, Na, or K) and 1 M MCF_3SO_3 (M = Li, Na, or K) in diethylene glycol dimethyl ether (DEGDME) were used as counter electrodes and electrolytes, respectively.

[a] *Department of Materials Science and Engineering, Research Institute of Advanced Materials (RIAM), Seoul National University, Gwanak-ro 599, Gwanak-gu, Seoul 151-742, Republic of Korea*
[b] *Center for Nanoparticle Research, Institute for Basic Science (IBS), Seoul National University, Gwanak-ro 599, Gwanak-gu, Seoul 151-742, Republic of Korea. E-mail: matlgen1@snu.ac.kr*

† Electronic supplementary information (ESI) available: Experimental and calculation details. See DOI: 10.1039/c6cc05362a

‡ Present address: Materials Science Division, Lawrence Berkeley National Laboratory, Berkeley, 94720 USA.

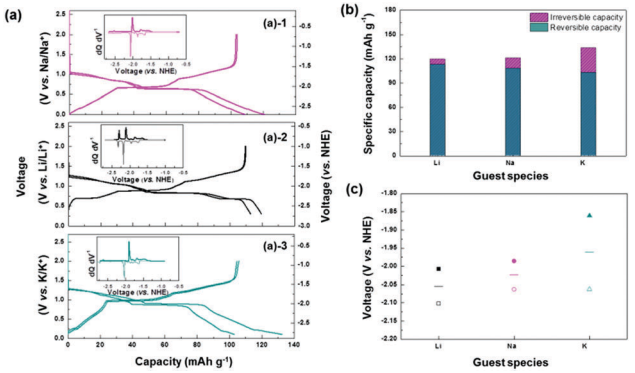

Fig. 1 Electrochemical properties of the graphite anode using DEGDME electrolytes. (a) Typical charge/discharge profiles of the graphite anode in the half-cell configurations (inset: $dQ\ dV^{-1}$ *vs.* voltage plots of graphite). (b) Specific capacity of the graphite anode obtained in alkali-ion cells. (c) Average voltages of graphite in alkali-ion cells (filled symbols: charge voltage, empty symbols: discharge voltage, lines: average voltage).

Note that we selected MCF_3SO_3 (M = Li, Na, or K) salts in this study because Li salts with other anions (such as PF_6, BF_4, and ClO_4) do not have (or have too low) solubility in DEGDME solvent and, in our comparative investigations among Li, Na and K, we wanted to rule out the unnecessary complications such as the anion contribution. Fig. 1(a) presents typical charge/discharge profiles of the graphite anode in Na ((a)-1), Li ((a)-2), and K ((a)-3) cells at a constant current of 10 mA g^{-1}. The electrochemical properties of the Na cell agree with a previous report;[12,13] however, it is noteworthy that the charge/discharge profiles of the K (*vs.* K/K^+) and Li (*vs.* Li/Li^+) insertions differ significantly from those observed for a graphite anode in conventional KIBs or LIBs.[4,6,18] The voltages differ by more than 1 V for both cases, with values of $\sim$0.2 V (*vs.* K/K^+) and $\sim$0.1 V (*vs.* Li/Li^+) for ion insertion in conventional KIBs or LIBs, respectively. Moreover, regardless of the alkali ion species, similar charge/discharge profiles were obtained for Na, Li, and K cells in terms of the overall shape and relative location of the voltage plateau, indicative of the common reaction mechanism for Na, K, and Li insertions.[19]

Fig. 1(b) shows that the observed capacities are comparable among the three cells. This finding is rather unexpected considering the substantial differences in the solubility limit of each alkali ion in graphite (LiC_6, KC_8, and $Na\delta C$ (δ~0)) as well as in their atomic weights (Li $\sim$6.941, Na $\sim$22.989, and K $\sim$39.098 g mol^{-1}). The origin of this phenomenon will be discussed later with respect to the insertion mechanism. Slightly increased irreversible capacity was observed for the Na and K insertions. The irreversible capacity in the initial discharge may originate from the decomposition of the electrolyte and formation of the solid–electrolyte interphase; however, further study is required. We further examined the alkali ion storage voltages in each cell by plotting the differential capacities ($dQ\ dV^{-1}$) *versus* voltage in the insets of Fig. 1(a). In each inset, we normalized the voltages to the NHE reference to selectively compare the storage potentials into graphite irrespective of the ionization energy of each alkali ion.[20] Because the voltage *vs.* M/M^+ includes the ionization energy contribution from M and the redox potential of Li/Li^+ differs (for example, from that of Na/Na^+ and K/K^+ by $\sim$0.3 and $\sim$0.1 V, respectively), the comparison of the voltage *vs.* NHE can be useful in evaluating the pure interaction between each alkali ion and the graphite host. Moreover, the relative stability of each ion insertion into the graphite host can be postulated from the voltages *vs.* NHE. Fig. 1(c) plots the voltages *vs.* NHE for Li, Na, and K during insertion and deinsertion, demonstrating that the average voltage of the graphite electrode increases when larger ions are intercalated (Li < Na < K). This finding implies that the Na or K insertions into the graphite host are energetically more favorable than Li insertions when disregarding the ionization energy of each alkali metal, in contrast to the conventional belief that Li-ion insertion into graphite would be much more favorable. The formation of K-intercalated graphite is inferred to be more stable compared with Na-intercalated or Li-intercalated graphite by 0.063 and 0.093 eV, respectively.

To understand the alkali ion storage mechanism in graphite, structural analysis was conducted using *ex situ* XRD upon discharge and charge processes. Fig. 2(a–c) show that graphite undergoes successive two-phase reactions during the electrochemical operation and forms layered intermediate phases in all three cases. The initial (002) peak from the pristine graphite splits into two peaks ((005) and (006)) arising from new intermediate phase I, followed by the evolution of new peaks ((004) and (005)) from intermediate phase II and finally a new set of peaks ((002) and (003)) from intermediate phase III. The interlayer distances (I_c) calculated for each intermediate phase are denoted in the XRD patterns in Fig. 2(a–c). The I_c values for the Na intercalated compounds in Fig. 2(b) are 18.45, 15.08, and 11.65 Å, which is consistent with a previous report on solvated Na ion intercalation.[13] However, the values for Li intercalated compounds in Fig. 2(a) are slightly smaller (18.00, 14.60, and 11.16 Å),

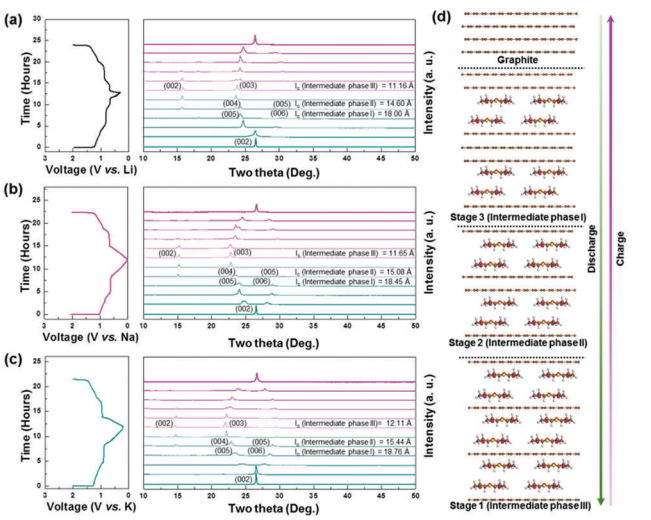

Fig. 2 Structural changes in graphite upon co-intercalation of alkali ion–ether solvent. The charge/discharge profiles and *ex situ* XRD patterns of graphite in (a) Li-, (b) Na-, and (c) K-ion cells. (d) Schematic of the alkali ion–solvent co-intercalation process in graphite *via* staging.

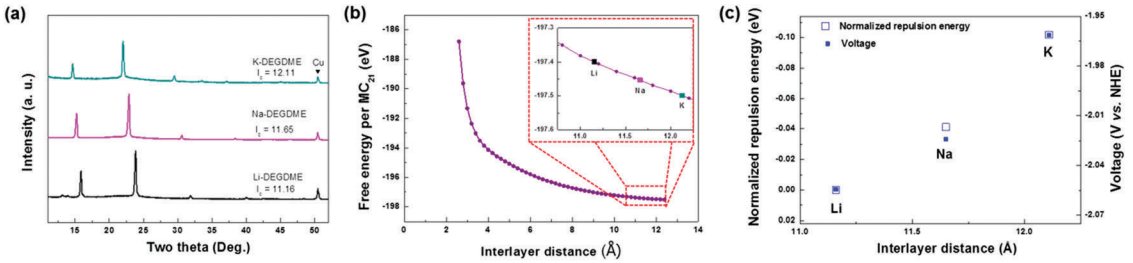

Fig. 3 Correlation between the structure of intercalant graphite and alkali ion storage potential. (a) *Ex situ* XRD patterns of intercalated graphite in Li-, Na-, and K-ion cells. (b) Free energy of the negatively charged graphite framework as a function of interlayer distance. The amount of injected charge is one per 21 C atoms. (Inset: magnification of region marked by a red square). (c) Plot of normalized repulsion energy and voltage as a function of interlayer distance (open squares: normalized repulsion energy, filled squares: voltage).

whereas those for K intercalated compounds (Fig. 2(c)) are larger (18.76, 15.44, and 12.11 Å), which most likely results from the different ionic sizes of Li^+ and K^+ compared with Na^+. Notably, the interlayer distances of the intermediate phases differ by ~3.4 Å for all three alkali ions, which corresponds to the interlayer distance of pristine graphite. This finding strongly suggests that the electrochemical alkali ion–ether solvent co-intercalation occurs through staging phenomena, where the intercalants occupy every n^{th} interlayer of graphite, leaving other interlayer spaces empty (stage n).[13] Fig. 2(d) illustrates possible staging sequences occurring during discharge, which is denoted as stage 3 to stage 1 based on the calculated interlayer distances of the intermediate phases. During the charging process (deinsertion), the XRD pattern recovers the pristine state of graphite following the opposite process of discharge, indicating reversible reactions. Fig. 3(a) compares the XRD patterns of the K, Na, or Li inserted discharge products, which clearly indicate that they are isostructurally layered compounds with slightly different interlayer distances (11.16, 11.65, and 12.11 Å for Li, Na, and K, respectively). Considering that (i) 11.65 Å corresponds to the interlayer distance for Na–ether co-intercalated graphite and (ii) the interlayer distances of each phase differ approximately by the size of the solvated ions,[13] it is evident that Li and K are intercalated in the form of solvated ions. The evidence of the solvated-ion intercalation for Li and K explains why substantially different voltages were observed compared with conventional LIBs or KIBs, where desolvated ion intercalation occurs. The comparable capacities and voltage profiles observed for the three cells are attributed to the bare interaction between the alkali ion and the graphite host being screened by the solvating molecules during the co-intercalation and being replaced to a large extent by the solvating molecule and graphite interaction.

To understand the stability of each co-intercalated graphite and elucidate the origin of the different voltages (*vs.* NHE) exhibited for the alkali ions, simple theoretical calculations were performed, as shown in Fig. 3(b) and (c). From the voltages measured in Fig. 1 (−1.961, −2.024, and −2.054 V *vs.* NHE for K, Na, and Li, respectively), it can be inferred that the K–ether co-intercalated graphite is more stable than its Li or Na counterparts by 93 and 63 meV, respectively. Several factors can affect the relative energy state of the intercalated graphite products. From the electrostatic perspective, these factors include (i) the attractive force between the cations and graphene layers, (ii) the repulsive force among the intercalated cations, and (iii) another repulsive term between the negatively charged graphene layers, whose relative dominance can be estimated from first-principles calculations. The first factor can be assessed by calculating Bader charges, which represents the amount of charge that each atom holds. In our calculations, the Bader charges were +0.88, +0.85, and +0.88 for ether-solvated Li, Na, and K ions, respectively. The similar values indicate that the attractive forces between these monovalent alkali ions and the negatively charged graphene host would be roughly the same for Li–, Na–, and K–ether co-intercalated systems and cannot be the dominant factor contributing to the higher stability of the K–ether co-intercalated phase. Similarly, the second parameter of the repulsion among cations would not be significantly different because of the comparable Bader charges. However, the repulsive term between the negatively charged graphene layers is expected to be sensitively affected by the species of intercalants in the discharged state, as observed by the different interlayer distances in Fig. 3(a) (11.16, 11.65, and 12.11 Å for Li, Na, and K intercalated phases, respectively).

The repulsive force and its contribution to the energy state of the discharge product can be estimated in relation to the interlayer distance, as shown in Fig. 3(b). Fig. 3(b) plots the free energy of a negatively charged graphite framework as a function of the interlayer distance, clearly revealing that the repulsion between negatively charged graphene layers decreases exponentially with the interlayer distance. We observed that the free energy reduction arising from the increase in the interlayer distance from Li to Na and K agrees remarkably well with the relative stability of the K–ether intercalated graphite. In the inset of Fig. 3(b), the interlayer distances of each alkali-ion-intercalated graphite system are indicated with the corresponding energies. When comparing these energies (normalized to the energy per carbon atom) with the observed voltages for each Li, Na, and K cell in Fig. 3(c), it is noted that the energy stabilization from the increase of the interlayer distance from Li to Na and K coincides with the potential difference observed in the galvanostatic measurements. The experimental voltage differences between the Li–ether and K–ether and between the Na–ether and K–ether were approximately 93 and 63 mV, respectively, as observed in Fig. 1(c), and these values agree well with the reduction of the

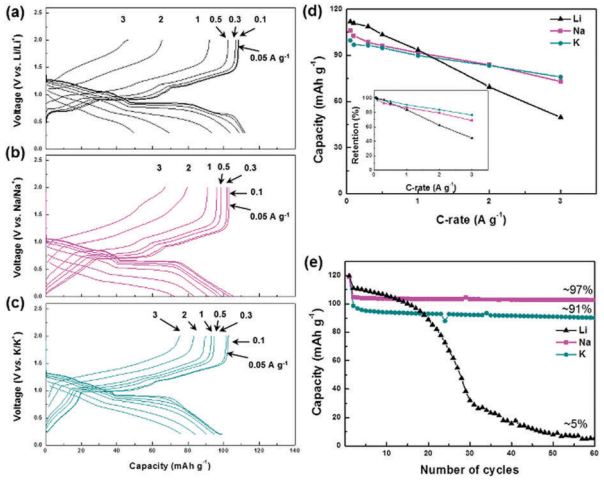

Fig. 4 Charge/discharge profiles at different current rates of (a) Li, (b) Na, and (c) K cells. (d) Rate capability (inset: retention) and (e) cycle stability of Li, Na, and K cells.

calculated free energies from the Li (or Na) to K case in Fig. 3(c). This finding strongly supports the idea that among the possible origins, the electrostatic contribution between negatively charged graphene layers in the discharged state and its sensitive variation with the interlayer distance is most likely the dominant reason for the different voltages observed for Li, Na, and K intercalation. A larger ion can most effectively stabilize the discharged graphite, thus leading to the higher potential.

We considered the practical feasibility of using DEGDME electrolytes in rechargeable batteries. When the ionic conductivity of DEGDME is compared with that of the conventional carbonate electrolyte, only a slight reduction is observed for DEGDME by approximately 10% (Fig. S1, ESI†). On the other hand, the characterization of the stability of electrolytes in a wide voltage window shows that DEGDME electrolyte provides much better oxidation stability than carbonate electrolyte particularly using $NaCF_3SO_3$ salts (Fig. S2, ESI†). The change of the salt to $NaClO_4$ could further stabilize the DEGDME electrolytes. It suggests that a DEGDME-based electrolyte system can be another plausible option for rechargeable batteries. In addition, we investigated the battery performance including rate capability and cycle stability. Fig. 4(a–c) shows the charge/discharge profiles of the graphite electrode in Li, Na, and K cells at various current rates from 0.05 to 3 A g^{-1}. When we compared the discharge capacities of the Li, Na, and K cells at increased current rates, higher rate capability is observed when larger ions are de/intercalated (Li < Na < K) as shown in Fig. 4(d). It indicates that larger ions move faster in the graphite electrode upon co-intercalation, which is attributable to the enlarged spaces between graphene layers while further experiments are required. Fig. 4(e) shows the cycle stability of the graphite electrode in Li, Na, and K cells. Na and K cells provide a stable cycle property up to 60 cycles (97% and 91% retention compared to the second cycle for Na and K, respectively) while the Li cell shows a rapid capacity degradation upon cycling.

Because the cycle stability is influenced by several factors including the stability of working electrodes (here, graphite), electrolytes, and counter electrodes, it is difficult to conclude what factors critically deteriorate the cycle life of Li cells, which will be further investigated in a future study.

In summary, we observed that various alkali ions (Li, Na, and K) can be intercalated into graphite in the form of solvated ions when DEGDME electrolyte is used. The intercalation behavior of each solvated alkali ion was clearly elucidated, and the staging phenomenon was commonly observed regardless of the alkali ion species. In this system, the interlayer distance increases proportionally with the cation size (Li < Na < K), which led to reduced repulsion between negatively charged graphene layers in the discharged state. The reduced repulsion in the larger solvated-ion graphite compound resulted in higher stability in the discharged state and, in turn, higher alkali ion storage potential. This systematic study on the insertion of various alkali ions into a graphite host broadens our understanding of intercalation chemistry in graphite and hints at an effective strategy to utilize graphite as a versatile host material for various rechargeable batteries.

This work was supported by (i) the Energy Efficiency & Resources of the Korea Institute of Energy Technology Evaluation and Planning (KETEP) grant funded by the Korean's government Ministry of Trade, Industry & Energy (MOTIE) (No. 20132020000270) and (ii) the Korea Institute of Energy Technology Evaluation and Planning (KETEP) and the Ministry of Trade, Industry & Energy (MOTIE) of the Republic of Korea (No. 20158510050040).

Notes and references

1 M.-S. Park, J.-H. Kim, Y.-N. Jo, S.-H. Oh, H. Kim and Y.-J. Kim, *J. Mater. Chem.*, 2011, **21**, 17960–17966.
2 Y. Yamada, K. Usui, C. H. Chiang, K. Kikuchi, K. Furukawa and A. Yamada, *ACS Appl. Mater. Interfaces*, 2014, **6**, 10892–10899.
3 J. Lee, M.-S. Park, Y.-S. Park, K.-N. Jung, J.-W. Lee, S. Y. Kim, Y. N. Jo, T. Yim, S.-M. Lee and Y.-J. Kim, *ChemElectroChem*, 2014, **1**, 1672–1678.
4 S. Komaba, T. Hasegawa, M. Dahbi and K. Kubota, *Electrochem. Commun.*, 2015, **60**, 172–175.
5 Z. Jian, W. Luo and X. Ji, *J. Am. Chem. Soc.*, 2015, **137**, 11566–11569.
6 W. Luo, J. Wan, B. Ozdemir, W. Bao, Y. Chen, J. Dai, H. Lin, Y. Xu, F. Gu, V. Barone and L. Hu, *Nano Lett.*, 2015, **15**, 7671–7677.
7 X.-F. Luo, C.-H. Yang, Y.-Y. Peng, N.-W. Pu, M.-D. Ger, C.-T. Hsieh and J.-K. Chang, *J. Mater. Chem. A*, 2015, **3**, 10320–10326.
8 Y. Liu, B. V. Merinov and W. A. Goddard, *Proc. Natl. Acad. Sci. U. S. A.*, 2016, **113**, 3735–3739.
9 Z. Wang, S. M. Selbach and T. Grande, *RSC Adv.*, 2014, **4**, 4069–4079.
10 Y. Okamoto, *J. Phys. Chem. C*, 2014, **118**, 16–19.
11 K. Nobuhara, H. Nakayama, M. Nose, S. Nakanishi and H. Iba, *J. Power Sources*, 2013, **243**, 585–587.
12 H. Kim, J. Hong, Y.-U. Park, J. Kim, I. Hwang and K. Kang, *Adv. Funct. Mater.*, 2015, **25**, 534–541.
13 H. Kim, J. Hong, G. Yoon, H. Kim, K.-Y. Park, M.-S. Park, W.-S. Yoon and K. Kang, *Energy Environ. Sci.*, 2015, **8**, 2963–2969.
14 B. Jache and P. Adelhelm, *Angew. Chem., Int. Ed.*, 2014, **53**, 10169–10173.
15 A. P. Cohn, K. Share, R. Carter, L. Oakes and C. L. Pint, *Nano Lett.*, 2015, **16**, 543–548.
16 Z. Zhu, F. Cheng, Z. Hu, Z. Niu and J. Chen, *J. Power Sources*, 2015, **293**, 626–634.
17 I. Hasa, X. Dou, D. Buchholz, Y. Shao-Horn, J. Hassoun, S. Passerini and B. Scrosati, *J. Power Sources*, 2016, **310**, 26–31.
18 Z. X. Shu, R. S. McMillan and J. J. Murray, *J. Electrochem. Soc.*, 1993, **140**, 922–927.
19 B. A. Jache, J. O. Binder, T. Abe and P. Adelhelm, *Phys. Chem. Chem. Phys.*, 2016, **18**, 14299–14316.
20 J. Muldoon, C. B. Bucur and T. Gregory, *Chem. Rev.*, 2014, **114**, 11683–11720.